Enhanced Skeletal Muscle Lipid Oxidative Efficiency in Insulin-Resistant vs Insulin-Sensitive Nondiabetic, Nonobese Humans

Jose E. Galgani, Karla Vasquez, Guillermo Watkins, Aude Dupuy, Justine Bertrand-Michel, Thierry Levade, and Cedric Moro

Department of Nutrition (J.E.G., K.V.), Faculty of Medicine, University of Chile, Santiago, Chile; Department of Nutrition, Diabetes, and Metabolism (J.E.G.) and School of Nutrition and Dietetics (J.E.G.), Faculty of Medicine, Pontifical Catholic University of Chile, Santiago, Chile; Department of Surgery (G.W.), Clinical Hospital J. J. Aguirre, University of Chile, Santiago, Chile; Institut National de la Santé et de la Recherche Médicale 1048 (A.D., J.B.-M.), Lipidomic Core Facility of Toulouse Metatoul Platform, and Laboratoire de Biochimie Métabolique (T.L.), Institut Fédératif de Biologie, Centre Hospitalier Universitaire Purpan, F-31059 Toulouse, France; Paul Sabatier University (A.D., J.B.-M., T.L., C.M.), F-31432 Toulouse, France; Institut National de la Santé et de la Recherche Médicale Unité Mixte de Recherche 1037 (T.L.), Cancer Research Center of Toulouse, and Institut National de la Santé et de la Recherche Médicale Unité Mixte de Recherche 1048 (C.M.), Obesity Research Laboratory, Institute of Metabolic and Cardiovascular Diseases (I2MC), F-31432 Toulouse, France

Context: Skeletal muscle insulin resistance is proposed to result from impaired skeletal muscle lipid oxidative capacity. However, there is no evidence indicating that muscle lipid oxidative capacity is impaired in healthy otherwise insulin-resistant individuals.

Objective: The objective of the study was to assess muscle lipid oxidative capacity in young, nonobese, glucose-tolerant, insulin-resistant vs insulin-sensitive individuals.

Design and Volunteers: In 13 insulin-sensitive [by Matsuda index (MI) (22.6 $\pm$ 0.6 [SE] kg/m^2); 23 $\pm$ 1 years; MI 5.9 $\pm$ 0.1] and 13 insulin-resistant (23.2 $\pm$ 0.6 kg/m^2; 23 $\pm$ 3 years; MI 2.2 $\pm$ 0.1) volunteers, skeletal muscle biopsy, blood extraction before and after an oral glucose load, and dual-energy x-ray absorptiometry were performed.

Main Outcome Measures: Skeletal muscle mitochondrial to nuclear DNA ratio, oxidative phosphorylation protein content, and citrate synthase and β-hydroxyacyl-CoA dehydrogenase activities were assessed. Muscle lipids and palmitate oxidation ($^{14}CO_2$ and ^{14}C-acid soluble metabolites production) at 4 [1-^{14}C]palmitate concentrations (45–520 μM) were also measured.

Results: None of the muscle mitochondrial measures showed differences between groups, except for a higher complex V protein content in insulin-resistant vs insulin-sensitive volunteers (3.5 $\pm$ 0.4 vs 2.2 $\pm$ 0.4; $P = .05$). Muscle ceramide content was significantly increased in insulin-resistant vs insulin-sensitive individuals ($P = .04$). Total palmitate oxidation showed a similar concentration-dependent response in both groups ($P = .69$). However, lipid oxidative efficiency (CO_2 to ^{14}C-acid soluble metabolites ratio) was enhanced in insulin-resistant vs insulin-sensitive individuals, particularly at the highest palmitate concentration (0.24 $\pm$ 0.04 vs 0.12 $\pm$ 0.02; $P = .02$).

Conclusions: We found no evidence of impaired muscle mitochondrial oxidative capacity in young, nonobese, glucose-tolerant, otherwise insulin-resistant vs insulin-sensitive individuals. Enhanced muscle lipid oxidative efficiency in insulin resistance could be a potential mechanism to prevent further lipotoxicity. **(*J Clin Endocrinol Metab* 98: E646–E653, 2013)**

ISSN Print 0021-972X ISSN Online 1945-7197
Printed in U.S.A.

Received August 17, 2012. Accepted January 11, 2013.
First Published Online February 7, 2013

Abbreviations: AUC, area under the curve; ASM, acid-soluble metabolite; CoA, coenzyme A; FAT, fatty acid translocase; GAPDH, glyceraldehyde-3-phosphate dehydrogenase; βHAD, β-hydroxyacyl-CoA dehydrogenase; mtDNA, mitochondrial DNA; NADH, nicotinamide adenine dinucleotide (reduced form).

Increased muscle lipid accumulation relates to insulin resistance in sedentary humans (1). A pressing question that remains unanswered is how lipids are accumulated in skeletal muscle of insulin-resistant individuals. Skeletal muscle lipid storage is determined by the balance between fatty acid uptake and oxidation. On the one hand, muscle fatty acid uptake appears to be unaffected in insulin resistance, considering that serum free-fatty acid concentration over 24 hours (2), adipose tissue glycerol turnover rate (3), and leg lipid uptake (4) were similar in insulin-sensitive vs. insulin-resistant individuals. On the other hand, insulin resistance has been characterized by reduced skeletal muscle mitochondrial density/capacity, which is postulated to lead to impaired lipid oxidation (5). Such evidence has become the basis accounting for skeletal muscle lipid accumulation and impaired insulin action (3, 6). Alternatively, impaired insulin signaling can also induce mitochondrial dysfunction (7). Finally, insulin resistance can be dissociated of impaired mitochondrial function. For instance, Zucker diabetic fatty rats showed preserved mitochondrial function during the development of diabetes (8). In turn, insulin resistance was unrelated to in vivo maximal mitochondrial function in type 2 diabetic subjects (9). Therefore, the role and relevance of mitochondrial capacity remains unclear in insulin resistance. This aspect becomes more controversial after noticing that lipid oxidation and insulin sensitivity can be augmented in the presence of skeletal muscle mitochondrial dysfunction (10).

In humans, further complexity to the interpretation relating insulin resistance, mitochondrial capacity (eg, morphology, number, activity, and gene expression), and lipid oxidation can be attributed to the inclusion of obese and/or type 2 diabetic individuals (4, 11–19). Both obesity and diabetes may influence fuel oxidation and bias the relationship between insulin resistance and lipid oxidation. Furthermore, skeletal muscle metabolism may respond differently depending of the stage of development of insulin resistance. In this respect, obesity and type 2 diabetes will be representative of later rather than earlier stages.

Studies in which obesity- and type 2 diabetes-unrelated insulin resistance has been evaluated, compared insulin-resistant individuals with family history of type 2 diabetes vs insulin-sensitive volunteers (3, 6). Although no assessment of skeletal muscle lipid oxidative capacity was performed, these studies found reduced skeletal muscle in vivo resting Krebs cycle flux and ATP synthesis rate in insulin resistance. Such findings were considered by the authors as indicative of skeletal muscle mitochondrial dysfunction.

Considering that skeletal muscle lipid oxidation has not been well documented in insulin resistance, the aim of the present study was to compare skeletal muscle mitochondrial oxidative capacity in young, nonobese, glucose-tolerant, insulin-sensitive and insulin-resistant individuals.

Methods and Procedures

Volunteers

Individuals were invited to participate by public advertising. At the screening visit, volunteers were healthy (by physical examination and routine laboratory tests), nonobese, and nonsmoking. They were not engaged in regular physical activity (>60 min/wk), and they had a sedentary lifestyle according to a physical activity questionnaire (20). They had stable body weight (change < 2 kg for the past 3 months), and none of them were under medication or hyper/hypocaloric diet.

A 75-g oral glucose tolerance test was performed in 60 volunteers. All had normal glucose tolerance according to the American Diabetes Association 2012 criteria. Volunteers having a Matsuda index (21) greater than 5.1 or less than 3.4 were classified as insulin sensitive or insulin resistant, respectively (Table 1). The protocol was approved by the Ethical Committee of the Faculty of Medicine, University of Chile, and volunteers provided written informed consent.

Experimental design

After screening, participants were instructed to avoid intense physical activity and maintain their usual diet for the 2 days preceding testing. On the testing day, a muscle biopsy was performed in overnight-fasted individuals. After that, 2 blood samples were taken 10 minutes apart, followed by a 75-g oral glucose load. Blood samples were drawn at 30, 60, 90, 120, 180, and 240 minutes after ingested the glucose. Then body composition was determined by dual-energy x-ray absorptiometry (Lunar DPX-L; Lunar Radiation Corp, Madison, Wisconsin).

Blood analysis

Serum glucose was measured by the glucose oxidase method, lactate by lactate oxidase method, free-fatty acid concentration by an enzymatic colorimetric method (NEFA-HR; Wako Chemicals, Richmond, Virginia), and insulin by direct chemiluminescent technology (Advia Centaur; Bayer Corp, Newbury, United Kingdom). Blood responses were calculated over 4 hours by the incremental area under the curve (AUC) using the trapezoidal method.

Muscle biopsy

Vastus lateralis muscle biopsies (350 mg) were obtained using a 5-mm Bergstrom needle. The skin, adipose tissue, and skeletal muscle fascia were anesthetized using 2% lidocaine solution (5 mL). A piece of the muscle was blotted, snap frozen, and stored in liquid nitrogen until assay. The remainder of the muscle was diluted in 1.7 mL of modified sucrose-EDTA medium (250 mM sucrose; 1 mM EDTA; 1 M Tris-HCl; and 2 mM ATP, pH 7.4) and maintained on ice.

Skeletal muscle palmitate oxidation

Muscle (~80 mg) was homogenized while maintained on ice in a glass tube containing modified sucrose-EDTA medium using

Table 1. Characteristics of Insulin-Sensitive and Insulin-Resistant Volunteers

	Insulin Sensitive		Insulin Resistant		
	Mean ± SE	Range	Mean ± SE	Range	*P* Value
Male/female	6/7		4/9		.42
Age, y	22.8 ± 0.6	19.8–26.3	23.0 ± 0.8	18.5–28.4	.79
Body mass, kg	62.8 ± 2.6	49.7–77.2	64.3 ± 3.1	49.8–83.7	.72
Height, m	1.66 ± 0.02	1.52–1.78	1.66 ± 0.02	1.54–1.80	.88
Body mass index, kg/m^2	22.6 ± 0.6	20.1–26.7	23.2 ± 0.6	19.5–26.5	.47
Body fat, %	20.7 ± 2.4	3.8–35.4	24.6 ± 1.7	11.8–33.0	.19
Arms fat, %	6.2 ± 0.5	3.9–10.5	7.0 ± 0.5	4.8–10.7	.29
Legs fat, %	39.5 ± 1.5	27.1–49.9	37.5 ± 1.3	30.0–45.4	.33
Trunk fat, %	46.0 ± 1.9	36.0–60.2	47.3 ± 1.4	37.1–56.3	.60
Fasting cholesterol, mg/dL	176 ± 8	145–226	169 ± 9	111–212	.55
Fasting triglycerides, mg/dL	78 ± 9	50–168	92 ± 12	50–195	.35
Fasting glucose mg/dL	88 ± 2	78–96	90 ± 2	76–104	.49
Fasting lactate, mmol/L	0.82 ± 0.06	0.50–1.30	1.15 ± 0.08	0.60–1.60	<.01
Fasting FFA, μmol/L	375 ± 47	96–696	354 ± 40	204–724	.73
Fasting insulin, mIU/mL	6.1 ± 0.3	4.5–8.1	15.9 ± 1.4	9.8–27.1	<.0001
2-Hour glucose, mg/dL	98 ± 5	71–134	113 ± 5	66–138	.06
Matsuda index	6.0 ± 0.1	5.2–6.6	2.2 ± 0.1	1.3–3.4	<.0001

FFA, free fatty acid.

a homogenizer (Glas Col, LLC, Terre Haute, Indiana). Palmitate was prepared on each testing day by combining labeled [10 μL of 1 μCi/mL [1-^{14}C]palmitate (Perkin Elmer, Waltham, Massachusetts)] and nonlabeled [17–200 μL of 20 μM palmitate (Sigma, St Louis, Missouri)] palmitate. Palmitate was complexed to fatty acid-free BSA (MP Biomedicals, Solon, Ohio) for 30 minutes (37°C) at a constant palmitate to BSA ratio (3:1). Palmitate oxidation was determined (triplicate) at 45, 90, 180, and 520 μM palmitate by measuring production of ^{14}C-labeled acid-soluble metabolites (ASMs) and $^{14}CO_2$ from the carboxyl carbon, by use of a custom-made 24-well microtiter plate. Reactions were initiated by adding 310 μL of the incubation buffer (pH 7.4) to 80 μL of homogenate. Incubation buffer also contained 102 mM sucrose, 80 mM potassium chloride, 10 mM potassium phosphate, 8 mM Tris-HCl, 2 mM ATP, 1 mM magnesium chloride hexahydrate, 1 mM L-carnitine, 1 mM dithiothreitol, 0.2 mM EDTA, 0.1 mM malate, 0.1 mM nicotinamide adenine dinucleotide, 0.05 mM coenzyme A, and 0.5% fatty acid-free BSA. After incubation (60 minutes, 37°C), reactions were terminated by adding 40 μL of 70% perchloric acid, and the CO_2 produced was trapped in 200 μL of 1 M NaOH added to adjacent wells. The acidified medium was stored overnight (4°C), and then ASMs were assayed in supernatants. Radioactivity of CO_2 and ASMs were determined by liquid scintillation counting and normalized for muscle wet weight (22). Leftover muscle homogenate was stored at −80°C for determination of enzymatic activities.

Citrate synthase activity

Muscle homogenates were diluted 5-fold with distilled water. Activity was measured at 37°C (duplicate) in 100 mM Tris-HCl (pH 8.3) assay buffer containing dithionitrobenzoic acid (1 mM in 100 mM Tris buffer) and oxaloacetate (10 mM in 100 mM Tris buffer). After an initial 2-minute absorbance reading at 412 nm, the reaction was initiated by adding 3 mM acetyl-coenzyme A (CoA). This allows the formation of citrate and CoA (reduced form), and the reduction of dithionitrobenzoic acid by CoA-SH to mercaptide ion. The appearance of mercaptide ion is read at 412 nm every 12 seconds for 7 minutes. Values were adjusted for total protein.

Mitochondrial DNA content

DNA was extracted from frozen muscle (DNeasy blood and tissue kit; QIAGEN, Valencia, California). Relative amounts of mitochondrial DNA (mtDNA) and nuclear DNA were determined by quantitative RT-PCR as described previously (23). The sequences for the primer sets used for determination of mtDNA for nicotinamide adenine dinucleotide (reduced form) (NADH) dehydrogenase subunit 1 (*ND1*) gene were: forward primer, CCCTAAAACCCGCCACATCT, and reverse primer, GAGCGATGGTGAGAGCTAAGGT. Nuclear DNA for the lipoprotein lipase (*LPL*) gene was: forward primer, CGAGTCGTCTTTCTCCTGATGAT, and reverse primer, TTCTGGATTCCAATGCTTCGA. Data were normalized by the $2^{(\Delta\Delta Ct)}$ method.

Western blot of muscle mitochondrial complexes

Muscle was homogenized in a buffer containing 50 mM HEPES (pH 7.4), 2 mM EDTA, 150 mM NaCl, 30 mM $NaPPO_4$, 10 mM NaF, 1% Triton X-100, 10 μL/mL protease inhibitor (Sigma), 10 μL/mL phosphatase I inhibitor (Sigma), 10 μL/mL phosphatase II inhibitor (Sigma), and 1.5 mg/mL benzamidine HCl (24). Homogenates were centrifuged for 25 minutes at 15 000 × *g*, and supernatants were stored at −80°C. Solubilized proteins (40 μg) were run on a 4%–12% SDS-PAGE (Bio-Rad Laboratories, Ivry-sur-Seine, France), transferred onto nitrocellulose membrane (Hybond ECL; Amersham Biosciences, Piscataway, New Jersey), and incubated with the primary antibody OXPHOS (MitoSciences, Eugene, Oregon). Subsequently, immunoreactive proteins were determined by enhanced chemiluminescence reagent (GE Healthcare, Indianapolis, Indiana) and visualized by exposure to Hyperfilm ECL (GE Healthcare). Glyceraldehyde-3-phosphate dehydrogenase (GAPDH) (Cell Signaling Technology, Beverly, Massachusetts) served as an internal control.

β-Hydroxyacyl-CoA dehydrogenase (βHAD) activity

In duplicate, 35 μL of muscle homogenate was added to 190 μL of a buffer containing 100 mM liquid triethanolamine, 5 mM

EDTA disodium salt hydrate, and 0.45 mM NADH. After a 2-minute stabilization period, 15 μL of 2 mM acetoacetyl-CoA was added, which initiated the oxidation of NADH to the oxidation of NADH. The change in absorbance was measured at 340 nm every 12 seconds for 6 minutes (37°C). The values were adjusted for total protein.

Skeletal muscle lipid determination

Triglycerides/diglycerides

Muscle was homogenized in 1 mL of methanol/5 mM EGTA [2:1 (vol/vol)] with FAST-PREP (MP Biochemicals). The equivalent of 0.3 mg of tissue was evaporated, dry pellets were dissolved in 0.2 mL of NaOH (0.1 M) overnight, and protein was measured (Bio-Rad Laboratories). Lipids corresponding to 2 mg of tissue were extracted (25) in dichloromethane/methanol/water [2.5:2.5:2.1 (vol/vol/vol)] in the presence of the internal standards (3 μg of stigmasterol, 3 μg of 1,3-dimyristine, 3 μg of cholesteryl heptadecanoate, and 20 μg of glyceryl trinonadecanoate). The dichloromethane phase was evaporated to dryness. Neutral lipids were separated over an SPE column (glass Chromabond pure silice, 200 mg; Macherey Nagel, Düren, Germany), and neutral lipids were eluted with chloroform-methanol [9:1 (vol/vol) 2 mL]. The organic phase was evaporated to dryness and dissolved in 20 μL of ethyl acetate. One microliter of the lipid extract was analyzed by gas-liquid chromatography (FOCUS system; Thermo Electron, San Jose, California) using a Zebron-1 Phenomenex fused silica capillary columns (5 m × 0.32 mm inner diameter, 0.50 μm film thickness). Oven temperature was programmed from 200°C to 350°C at a rate of 5°C/min, and the carrier gas was hydrogen (0.5 bar). The injector and the detector were at 315°C and 345°C, respectively.

Acyl-carnitines

Muscle (10 mg) was homogenized in KH_2PO_4 buffer (pH 7.4), and then 20 μL of the homogenate was spotted on filter membranes (Protein Saver 903 cards; Whatman, Middlesex, United Kingdom). The dried spots were then treated as previously described (26). Data were acquired using a Micromass Quattro Micro API spectrometer equipped with a 2795 HPLC module (Waters, Milford, Massachusetts).

Ceramides

Total lipid corresponding to 5 mg of tissue was extracted (25) in chloroform-methanol-water [2.5:2.5:2.1 (vol/vol/vol)] in the presence of the internal standard ceramide NC15 (2 μg). Standards and sample solutions were analyzed using an Agilent 1290 UPLC system coupled to a G6460 triple quadripole spectrometer (Agilent Technologies, Palo Alto, California) and using MassHunter software (Agilent Technologies) for data acquisition and analysis. A UPLC Acquity BEH C8 column (100 × 2.1 mm, 1.7 μm; Waters) was used for liquid chromatography separations. The column temperature was controlled at 40°C. The mobile phase A was isopropanol/MeOH/H_2O [5:1:4 (vol/vol/vol)] + 0.2% formic acid + 0.028% NH_4OH; and mobile phase B was isopropanol + 0.2% formic acid + 0.028% NH_4OH. The gradient was as follows: from 30% to 100% B in 10 minutes; 10–12 minutes reach to 100% B in 2 minutes; and then back to 30% B in 1 minute for 1 minute reequilibrium prior to the next injection. The flow rate of the mobile phase was 0.3 mL/min and the injection volume was 5 μL. An electrospray source was used in the positive ion mode. A precursor ion scan was performed to obtain the different species' mass, and then the corresponding multiple reaction monitoring was used to quantify the different Cer d18:1 species. The areas of LC peaks were determined using QqQ Quantitative analysis software (Agilent Technologies).

Statistical analysis

Data are presented as mean ± SE. Analyses were performed using SAS version 9.2 (SAS Institute, Cary, North Carolina). The frequency of males and females in each group were compared by χ^2 test. Differences between groups were assessed by unpaired Student's *t* tests. Time effects were analyzed using 2-way, repeated-measures ANOVA. We also considered the influence of sex and sex × group interaction by ANOVA. The statistical significance for multiple comparisons was adjusted with the Tukey-Kramer method. A value of $P < .05$ was considered significant.

Results

Volunteers' characteristics at the screening visit are shown in Table 1. Insulin-resistant and insulin-sensitive groups included similar proportion of males and females, age, body mass index, body fat mass, and fat distribution. Similarly, serum fasting glucose and lipid concentrations showed no differences, whereas 2 hours after glucose ingestion, glycemia tended to be higher in insulin-resistant vs insulin-sensitive individuals ($P = .06$). Insulin sensitivity, determined by the Matsuda index, was on average about 3-fold higher in insulin-sensitive vs insulin-resistant individuals. We found no influence of sex and sex × group interaction on the outcomes assessed.

Serum glucose, lactate, free-fatty acid, and insulin response to an oral glucose load

Serum glucose response evaluated over 4 hours as the incremental AUC was similar between insulin-sensitive and insulin-resistant individuals (624 ± 20 vs 679 ± 30 mg/min · dL, respectively; $P = .14$), whereas insulin AUC was 299 ± 23 and 550 ± 79 and mIU/min · mL, respectively ($P < .01$). Insulin-resistant vs insulin-sensitive individuals showed increased serum lactate concentration both in fasting (Table 1) as well as after glucose ingestion (4 hour incremental AUC: 8.5 ± 0.3 vs 7.2 ± 0.4 mmol/min · L; $P = .03$). Serum fasting free-fatty acid concentration (Table 1) as well as their suppression after 60 minutes of glucose ingestion ($P = .99$) was similar between groups.

Skeletal muscle lipid content

Because lipid accumulation in skeletal muscle is associated with insulin resistance, we determined the content of triglycerides and putative bioactive lipids involved in insulin resistance. As shown in Figure 1, we found no difference between groups for muscle triglycerides, total

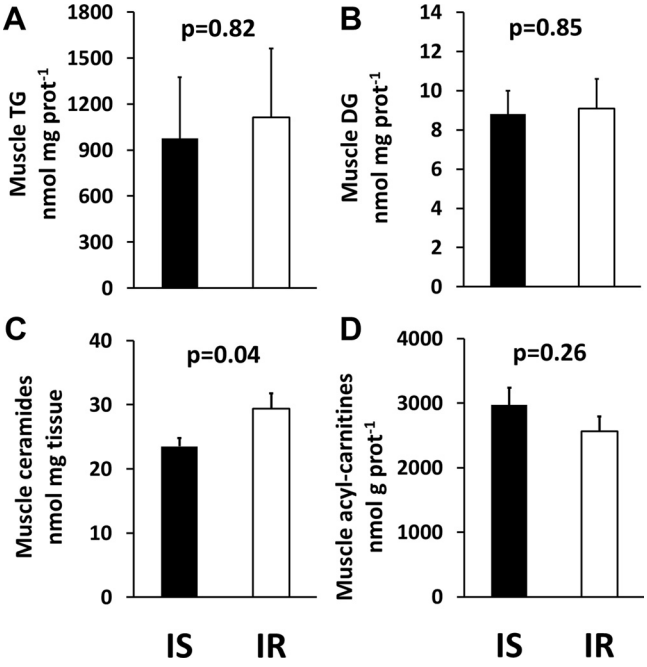

Figure 1. Skeletal muscle lipid content in insulin-sensitive and insulin-resistant volunteers. Triglycerides (A), total diglycerides (B), total ceramides (C), and total acyl-carnitines (D) are shown. IR, insulin resistant; IS, insulin sensitive.

diglycerides and total acyl-carnitine contents, whereas the total ceramide content was increased in insulin-resistant vs insulin-sensitive individuals (1.25-fold, $P = .04$). In addition, when analysis of acyl-carnitines was carried out for every species, a trend for lower acetyl-carnitine content was detected in insulin-resistant vs insulin-sensitive individuals ($P = .08$, Supplemental Table 1, published on The Endocrine Society's Journals Online web site at http://jcem.endojournals.org).

Skeletal muscle mitochondrial characteristics

Three common surrogates of muscle mitochondrial density/capacity were assessed in this study, ie, mitochondrial to nuclear DNA ratio, citrate synthase activity, and mitochondrial protein complex content (Table 2 and Supplemental Figure 1). No differences were observed between groups, except for complex V protein content, which was about 1.5-fold higher in insulin-resistant vs insulin-sensitive individuals.

The activity of βHAD, a main intramitochondrial enzyme participating in long-chain fatty acid catabolism, did not change between groups (Table 2).

Skeletal muscle palmitate oxidation rate

Palmitate oxidation ($^{14}CO_2$ and ^{14}C-ASM production) increased as a function of the palmitate concentration ($P < .01$; Figure 2, A and B). When palmitate oxidation was compared between groups, $^{14}CO_2$ and ^{14}C-ASM production rates were similar ($P = .33$–$.76$; Figure 2, A and B). The CO_2 to ASM ratio, a marker of mitochondrial lipid oxidative efficiency, differed among palmitate concentrations ($P = .001$) and between groups ($P = .02$), with a borderline interaction between concentration and group ($P = .07$; Figure 2C). Indeed, increased lipid oxidative efficiency was observed in insulin-resistant vs insulin-sensitive individuals, particularly at the highest palmitate concentration (0.24 ± 0.04 vs 0.12 ± 0.02, $P = .02$; Figure 2C).

Table 2. Skeletal Muscle Mitochondrial Capacity Markers in Insulin-Sensitive and Insulin-Resistant Volunteers

	Insulin Sensitive	Insulin Resistant	*P* Value
Complex I	3.33 ± 0.40	2.88 ± 0.35	.42
Complex II	3.05 ± 0.41	2.35 ± 0.24	.19
Complex III	1.39 ± 0.15	1.50 ± 0.20	.63
Complex IV	3.72 ± 0.45	3.33 ± 0.45	.55
Complex V	2.21 ± 0.43	3.46 ± 0.41	.05
mtDNA/nDNA	172 ± 21	199 ± 27	.42
Citrate synthase activity, nmol/mg protein^{-1} per minute^{-1}	30.2 ± 2.0	29.6 ± 1.9	.81
βHAD activity, nmol/mg protein^{-1} minute^{-1}	1.00 ± 0.06	0.87 ± 0.07	.18

Abbreviation: nDNA, nuclear DNA. Insulin-sensitive and insulin-resistant individuals were defined by the Matsuda index as higher than 5.1 or lower than 3.4, respectively. Mitochondrial complexes were normalized to glyceraldehyde-3-phosphate dehydrogenase protein content (dimensionless values); mtDNA/nDNA, mitochondrial to nuclear DNA ratio (dimensionless values).

Discussion

We found no evidence of impaired skeletal muscle mitochondrial oxidative capacity in insulin-resistant vs insulin-sensitive individuals. In fact, insulin resistance was characterized by an enhanced complete to incomplete palmitate oxidation ratio, particularly evident at the highest palmitate concentration. This suggests that skeletal muscle from insulin-resistant young individuals compensated the increase in palmitate supply by increasing the lipid oxidative efficiency.

Our findings do not support previous observations indicating that insulin resistance is associated with impaired muscle mitochondrial oxidative capacity (4, 11–17). Such contrasting outcome may be attributed to the fact that only nonobese, young individuals with and without insulin resistance were included in this study. Both groups showed similar fasting glycemia and insulin-resistant vs insulin-sensitive individuals had slightly higher (not significant) postprandial glucose response, suggesting that our insulin-resistant volunteers were at their early stage of

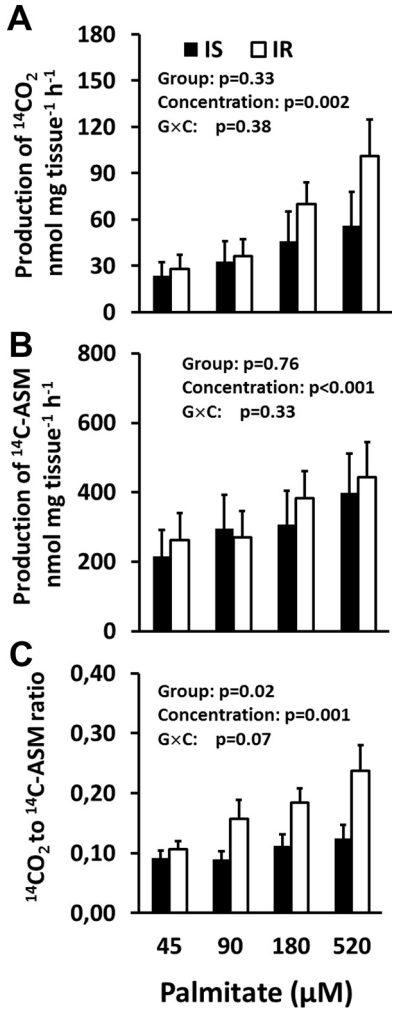

Figure 2. Skeletal muscle homogenate palmitate oxidation in insulin-sensitive and insulin-resistant volunteers. Complete oxidation ($^{14}CO_2$) (A); incomplete oxidation (^{14}C-acid soluble metabolites) (B); and complete-to-incomplete palmitate oxidation ratio (C) are shown. All experiments were performed using 1 μCi/ml [1-^{14}C]palmitate. G × C, group-concentration interaction; IR, insulin resistant; IS, insulin sensitive.

the insulin resistance development. Thus, studies reporting decreased muscle lipid oxidation (4, 19), citrate synthase activity (11), or mitochondrial respiration (12, 13) in insulin resistance may be biased by the presence of obesity and/or type 2 diabetes.

Lack of agreement between our findings and previous reports may be influenced by the method used to assess skeletal muscle mitochondrial density/capacity. For instance, this and other (27) studies found similar skeletal muscle mitochondrial density (by mtDNA content) in insulin-sensitive vs insulin-resistant individuals. However, when muscle mitochondrial density was determined by electron microscopy, reduced mitochondrial content was observed in insulin resistance (27).

The presence of a family history of type 2 diabetes may also play a role on explaining such divergent findings. In this regard, young, nonobese, healthy, insulin-resistant individuals with type 2 diabetes family background showed reduced in vivo resting skeletal muscle Krebs cycle flux when compared with well-matched insulin-sensitive volunteers (6), whereas we observed similar ex vivo citrate synthase activity (rate limiting Krebs cycle enzyme) in insulin-sensitive vs insulin-resistant individuals without a reported family history of type 2 diabetes. Our ex vivo enzymatic assay is indicative of the maximal citrate synthase activity, whereas the in vivo resting metabolic assay is performed under submaximal conditions. Taken together, such results may suggest that oxidative capacity is preserved in insulin resistance, at least at early stages. In turn, reduced Krebs cycle flux reported in insulin resistance may be due to decreased skeletal muscle ATP demand (28). Indeed, in vivo resting skeletal muscle ATP synthesis rate is lowered in insulin-resistant individuals with a family history of type 2 diabetes (3). Although this finding has been interpreted as indicative of mitochondrial dysfunction, we support the hypothesis that skeletal muscle energy demand may be reduced in insulin resistance.

Alternatively, nonoxidative glycolytic metabolism might be enhanced in insulin resistance, which will decrease the activity of oxidative pathways. In fact, in the present and other studies (29), serum fasting and postprandial lactate concentration was increased in insulin-resistant individuals. Although skeletal muscle is the main tissue releasing and taking up lactate (30), we cannot be conclusive about the role of skeletal muscle as a source of increased serum lactate concentration in insulin resistance.

Koves et al (31) provided evidence indicating that fatty acid intermediates may accumulate when lipid oxidative efficiency is reduced, which can negatively affect insulin signaling. We propose that enhanced muscle lipid oxidative efficiency observed in insulin-resistant individuals, particularly when exposed to a high lipid supply, may be a compensatory mechanism to prevent further lipid accumulation and alleviate insulin resistance, particularly at the early stages of the condition. In this regard, obesity-related insulin resistance, ie, chronic overnutrition, is characterized by reduced skeletal muscle lipid oxidative efficiency (31).

Our findings may also be affected by the intrinsic conditions of our ex vivo approach. First, we incubated the muscle homogenate with a carboxyl-terminal labeled palmitate, and then we can detect only CO_2 and ASM derived from that carbon. Thus, potential defects in medium- and short-chain fatty acid oxidation may not be detected. Future studies using [U-^{14}C]palmitate could be helpful to investigate this issue. Second, it is also proposed that insulin-resistant or diabetic states are characterized

by insufficient supply of carbons to Krebs cycle, which would limit complete oxidation and lead to accumulation of acyl-carnitines (32). Because our ex vivo experimental approach provides sufficient anaplerotic substrates, our findings could not apply to in vivo conditions. However, the fact that total acyl-carnitines content was not increased in the muscle of insulin-resistant individuals might be indicative that enhanced lipid oxidative efficiency may proceed in in vivo conditions. Furthermore, findings from an in vivo metabolomic study showed that obese, type 2 diabetic young vs nonobese young individuals had enhanced fatty acid oxidative capacity (33), which highlights the fact that metabolic response may differ during the time course of the development of insulin resistance. Third, fatty acid concentration remaining in muscle samples could differentially dilute added palmitate. However, such a factor should not affect the CO_2 to ASM ratio, so our findings may still remain valid.

Lipid oxidative efficiency measured in human muscle cells from obese and lean donors, and after overexpression of fatty acid translocase (FAT)/CD36 protein (a sarcolemmal fatty acid translocase) in muscle cells from lean donors may support the role of the stage of insulin resistance (34). In this regard, muscle cells from obese vs lean donors showed increased fatty acid uptake and FAT/CD36 protein content as well as lower complete fatty acid oxidation, higher incomplete oxidation, and consequently reduced lipid oxidative efficiency. When FAT/CD36 protein was overexpressed in muscle cells from lean donors, a condition resembling the condition observed in muscle cells from obese donors, fatty acid uptake and complete and incomplete oxidation were increased, whereas lipid oxidative efficiency was preserved (34).

These results may suggest that increased lipid uptake in muscle cells obtained from a hormonal/nutrient environment characterized by chronic overnutrition (ie, obese donors) shows impaired ability to adjust its lipid oxidative efficiency (34). On the contrary, an acute increase in lipid influx in muscle cells from lean donors did not impair lipid oxidative efficiency (34), which supports the idea that mitochondrial abnormalities may be triggered at later stages of insulin resistance. In the same line, humans overfed for 1 month developed insulin resistance; however, markers of mitochondrial content and function remained unchanged (35).

Based on the similar muscle triglyceride, diglyceride, and acyl-carnitine content between groups, we may anticipate a comparable muscle lipid uptake in insulin resistance. However, insulin-resistant vs insulin-sensitive individuals showed increased muscle ceramide content, which can also be augmented in response to lipid oversupply (36). Additionally, we observed similar serum lipid (triglyceride and free fatty acid) concentration between groups, which is consistent with evidence comparing serum free-fatty acid concentration over 24 hours in individuals with and without insulin resistance (2). Still, we cannot exclude that muscle lipid uptake may be different between insulin-resistant and insulin-sensitive individuals.

In conclusion, isolated insulin resistance, as found in young, healthy, glucose-tolerant, nonobese individuals, was not characterized by impaired muscle mitochondrial oxidative capacity. Indeed, muscle efficiency for lipid oxidation appears to be enhanced in insulin resistance, particularly in a condition of high lipid supply, which appeared to prevent further accumulation of muscle acyl-carnitines. The assessment of muscle mitochondrial capacity and lipid oxidation as a function of the stage of insulin resistance development will provide further insight about the mechanisms leading to muscle lipid accumulation and impaired insulin action in humans.

Acknowledgments

We express our appreciation to the participants. We thank to Juana Codoceo, BSc, Camila Pierart, MD, and Katie Louche, BSc (I2MC) for their outstanding assistance. We also thank M. Auriol and L. Fernandez (Laboratoire de Biochimie Métabolique, Centre Hospitalier Universitaire Toulouse, Toulouse, France) for lipidomic analyses, advice, and technical assistance.

Address all correspondence and requests for reprints to: Jose E. Galgani, PhD, Department of Nutrition, Diabetes, and Metabolism, Faculty of Medicine, Pontifical Catholic University of Chile, Alameda, 340 Santiago, Chile. E-mail: jgalgani@uc.cl.

This work was supported by the Chilean Commission of Science and Technology, Fondecyt 11090007 (to J.E.G.) and European Foundation for the Study of Diabetes/Novo Nordisk-France (to C.M.).

Disclosure Summary: The authors declare that there is no duality of interest associated with this manuscript.

References

1. **Moro C, Galgani JE, Luu L, et al.** Influence of gender, obesity, and muscle lipase activity on intramyocellular lipids in sedentary individuals. *J Clin Endocrinol Metab*. 2009;94:3440–3447.
2. **Nyholm B, Walker M, Gravholt CH, et al.** Twenty-four-hour insulin secretion rates, circulating concentrations of fuel substrates and gut incretin hormones in healthy offspring of type II (non-insulin-dependent) diabetic parents: evidence of several aberrations. *Diabetologia*. 1999;42:1314–1323.
3. **Petersen KF, Dufour S, Befroy D, Garcia R, Shulman GI.** Impaired mitochondrial activity in the insulin-resistant offspring of patients with type 2 diabetes. *N Engl J Med*. 2004;350:664–671.
4. **Kelley DE, Goodpaster B, Wing RR, Simoneau JA.** Skeletal muscle fatty acid metabolism in association with insulin resistance, obesity, and weight loss. *Am J Physiol*. 1999;277:E1130–E1141.

5. **Turner N, Heilbronn LK.** Is mitochondrial dysfunction a cause of insulin resistance? *Trends Endocrinol Metab*. 2008;19:324–330.
6. **Befroy DE, Petersen KF, Dufour S, et al.** Impaired mitochondrial substrate oxidation in muscle of insulin-resistant offspring of type 2 diabetic patients. *Diabetes*. 2007;56:1376–1381.
7. **Sleigh A, Raymond-Barker P, Thackray K, et al.** Mitochondrial dysfunction in patients with primary congenital insulin resistance. *J Clin Invest*. 2011;121:2457–2461.
8. **De Feyter HM, Lenaers E, Houten SM, et al.** Increased intramyocellular lipid content but normal skeletal muscle mitochondrial oxidative capacity throughout the pathogenesis of type 2 diabetes. *FASEB J*. 2008;22:3947–3955.
9. **Bajpeyi S, Pasarica M, Moro C, et al.** Skeletal muscle mitochondrial capacity and insulin resistance in type 2 diabetes. *J Clin Endocrinol Metab*. 2011;96:1160–1168.
10. **Handschin C, Choi CS, Chin S, et al.** Abnormal glucose homeostasis in skeletal muscle-specific PGC-1α knockout mice reveals skeletal muscle-pancreatic β cell crosstalk. *J Clin Invest*. 2007;117:3463–3474.
11. **Kelley DE, He J, Menshikova EV, Ritov VB.** Dysfunction of mitochondria in human skeletal muscle in type 2 diabetes. *Diabetes*. 2002;51:2944–2950.
12. **Mogensen M, Sahlin K, Fernstrom M, et al.** Mitochondrial respiration is decreased in skeletal muscle of patients with type 2 diabetes. *Diabetes*. 2007;56:1592–1599.
13. **Phielix E, Schrauwen-Hinderling VB, Mensink M, et al.** Lower intrinsic ADP-stimulated mitochondrial respiration underlies in vivo mitochondrial dysfunction in muscle of male type 2 diabetic patients. *Diabetes*. 2008;57:2943–2949.
14. **Ritov VB, Menshikova EV, Azuma K, et al.** Deficiency of electron transport chain in human skeletal muscle mitochondria in type 2 diabetes mellitus and obesity. *Am J Physiol Endocrinol Metab*. 2010;298(1):E49–E58.
15. **Ritov VB, Menshikova EV, He J, Ferrell RE, Goodpaster BH, Kelley DE.** Deficiency of subsarcolemmal mitochondria in obesity and type 2 diabetes. *Diabetes*. 2005;54:8–14.
16. **Patti ME, Butte AJ, Crunkhorn S, et al.** Coordinated reduction of genes of oxidative metabolism in humans with insulin resistance and diabetes: potential role of PGC1 and NRF1. *Proc Natl Acad Sci USA*. 2003;100:8466–8471.
17. **Giebelstein J, Poschmann G, Hojlund K, et al.** The proteomic signature of insulin-resistant human skeletal muscle reveals increased glycolytic and decreased mitochondrial enzymes. *Diabetologia*. 2012;55:1114–1127.
18. **Kelley DE, Simoneau JA.** Impaired free fatty acid utilization by skeletal muscle in non-insulin-dependent diabetes mellitus. *J Clin Invest*. 1994;94:2349–2356.
19. **Bandyopadhyay GK, Yu JG, Ofrecio J, Olefsky JM.** Increased malonyl-CoA levels in muscle from obese and type 2 diabetic subjects lead to decreased fatty acid oxidation and increased lipogenesis; thiazolidinedione treatment reverses these defects. *Diabetes*. 2006;55:2277–2285.
20. **Hagstromer M, Oja P, Sjostrom M.** The International Physical Activity Questionnaire (IPAQ): a study of concurrent and construct validity. *Public Health Nutr*. 2006;9:755–762.
21. **Matsuda M, DeFronzo RA.** Insulin sensitivity indices obtained from oral glucose tolerance testing: comparison with the euglycemic insulin clamp. *Diabetes Care*. 1999;22:1462–1470.
22. **Veerkamp JH, van Moerkerk TB, Glatz JF, Zuurveld JG, Jacobs AE, Wagenmakers AJ.** 14CO2 production is no adequate measure of [14C]fatty acid oxidation. *Biochem Med Metab Biol*. 1986;35:248–259.
23. **Sparks LM, Moro C, Ukropcova B, et al.** Remodeling lipid metabolism and improving insulin responsiveness in human primary myotubes. *PLoS One*. 2011;6:e21068.
24. **Badin PM, Louche K, Mairal A, et al.** Altered skeletal muscle lipase expression and activity contribute to insulin resistance in humans. *Diabetes*. 2011;60:1734–1742.
25. **Bligh EG, Dyer WJ.** A rapid method of total lipid extraction and purification. *Can J Biochem Physiol*. 1959;37:911–917.
26. **Attane C, Foussal C, Le Gonidec S, et al.** Apelin treatment increases complete fatty acid oxidation, mitochondrial oxidative capacity, and biogenesis in muscle of insulin-resistant mice. *Diabetes*. 2012;61:310–320.
27. **Morino K, Petersen KF, Dufour S, et al.** Reduced mitochondrial density and increased IRS-1 serine phosphorylation in muscle of insulin-resistant offspring of type 2 diabetic parents. *J Clin Invest*. 2005;115:3587–3593.
28. **Holloszy JO.** Skeletal muscle "mitochondrial deficiency" does not mediate insulin resistance. *Am J Clin Nutr*. 2009;89:463S–466S.
29. **Lovejoy J, Newby FD, Gebhart SS, DiGirolamo M.** Insulin resistance in obesity is associated with elevated basal lactate levels and diminished lactate appearance following intravenous glucose and insulin. *Metabolism*. 1992;41:22–27.
30. **Consoli A, Nurjahan N, Gerich JE, Mandarino LJ.** Skeletal muscle is a major site of lactate uptake and release during hyperinsulinemia. *Metabolism*. 1992;41:176–179.
31. **Koves TR, Ussher JR, Noland RC, et al.** Mitochondrial overload and incomplete fatty acid oxidation contribute to skeletal muscle insulin resistance. *Cell Metab*. 2008;7:45–56.
32. **Fiehn O, Garvey WT, Newman JW, Lok KH, Hoppel CL, Adams SH.** Plasma metabolomic profiles reflective of glucose homeostasis in non-diabetic and type 2 diabetic obese African-American women. *PLoS One*. 2010;5:e15234.
33. **Mihalik SJ, Michaliszyn SF, de las Heras J, et al.** Metabolomic profiling of fatty acid and amino acid metabolism in youth with obesity and type 2 diabetes: evidence for enhanced mitochondrial oxidation. *Diabetes Care*. 2012;35:605–611.
34. **Bell JA, Reed MA, Consitt LA, et al.** Lipid partitioning, incomplete fatty acid oxidation, and insulin signal transduction in primary human muscle cells: effects of severe obesity, fatty acid incubation, and fatty acid translocase/CD36 overexpression. *J Clin Endocrinol Metab*. 2010;95:3400–3410.
35. **Samocha-Bonet D, Campbell LV, Mori TA, et al.** Overfeeding reduces insulin sensitivity and increases oxidative stress, without altering markers of mitochondrial content and function in humans. *PLoS One*. 2012;7:e36320.
36. **Chavez JA, Summers SA.** A ceramide-centric view of insulin resistance. *Cell Metab*. 2012;15:585–594.